参赛学生姓名: 陈思睿

中学: 北京师范大学附属实验中学

省份: 北京市

国家/地区:中国

指导老师姓名: 孙晓明

指导老师单位: 北京化工大学

指导老师姓名: 孔婀静

指导老师单位: 北京师范大学附属实验中学

论文题目: Fluoride-Ion Triggers Stable and Active Seawater Oxidation at 1A/cm<sup>2</sup>

# Fluoride-Ion Triggers Stable and Active Seawater Oxidation at 1A/cm<sup>2</sup>

Researcher: Sirui Chen

Experimental High School attached to Beijing Normal University

Tutor: Professor Xiaoming Sun

Beijing University of Chemical Technology

Tutor: Ejing Kong

Experimental High School attached to Beijing Normal University

# **Abstract**

Cl<sup>-</sup> poisoning and corrosion of the anode remain major challenges in seawater electrolysis, often requiring complex electrode designs that limit scalability. In this work, a simple electrolyte engineering strategy was proposed. By simply adding 0.25 M F<sup>-</sup> to saline electrolyte, traditional NiFe layered double hydroxide (NiFe-LDH) anodes not only exhibited high OER performance but also maintained corrosion-free operation at 1 A cm<sup>-2</sup> for 1500 hours, such performance is comparable to that of many advanced anodes specifically designed for seawater electrolysis. Comprehensive characterizations confirmed that the added F<sup>-</sup> dynamically adsorbed onto the NiFe-LDH surface, triggering charge redistribution and accelerating structural reconstruction, which boosted OER activity. Additionally, the inherently high charge localization of F<sup>-</sup> played a crucial role in repelling Cl<sup>-</sup> through electrostatic interaction, serving as a protective barrier that significantly enhanced the corrosion resistance during operation. This simple electrolyte engineering strategy provides a practical and scalable solution for advancing seawater electrolysis.

# **Keywords**

Seawater electrolysis; corrosion resistance; oxygen evolution reaction; fluoride; electrolyte engineering

# Catalogue

Abstract	3
Keywords	3
1. Introduction	5
2. Results	6
3. Conclusion	1
4. Methods1	2
4.1 Chemicals and materials1	2
4.2 Synthesis of NiFe LDHs electrode1	2
4.3 Physical characterization1	2
4.4 Electrochemical measurements1	3
4.5 In-situ electrochemical Raman measurements1	3
5. Acknowledgements	4
6. References	5

#### 1. Introduction

Hydrogen energy is a crucial component of the future clean energy system<sup>[1]–[3]</sup>. Using seawater as a feedstock for electrolysis enables hydrogen production while conserving scarce freshwater resources and contributing to energy decarbonization<sup>[4]–[7]</sup>. However, the complex composition of seawater, particularly the presence of Cl<sup>-</sup>, significantly impairs the oxygen evolution reaction (OER) activity at the anodes and leads to their corrosion<sup>[8]–[10]</sup>.

Recent efforts have been devoted to designing anodes that combine excellent OER performance with enhanced durability against corrosion[11]-[16]. Liu et al developed a RuNiMo catalyst that generated MoO<sub>4</sub><sup>2-</sup> during seawater oxidation, forming an electrostatic barrier to Cl<sup>-</sup> and enabling continuous operation at 0.5 A cm<sup>-2</sup> for 3000 hours with an overpotential ( $\eta_{500}$ ) around 400 mV<sup>[17]</sup>. Lu et al proposed a "sulfate ion immobilization" by constructing a NiFeBa layered double hydroxides (LDH) catalyst assisted with additional SO<sub>4</sub><sup>2-</sup> in the electrolyte, which maintained the high intrinsic activity of NiFe while repelling Cl-, achieving over 10000 hours of stability at 0.4 A cm<sup>-2</sup> in an alkaline seawater electrolyte[18]. Our team also developed a series of chloride-repelling anodes based on anion engineering, including NiFe/NiSx-Ni foam[9], CoFe Prussian blue analogue/Co<sub>2</sub>P[10], and CoFeAl-LDH<sup>[19]</sup>. These materials release functional anions such as  $SO_4^{2-}$ ,  $Fe(CN)_6^{3-}$ ,  $PO_4^{3-}$ , and  $Al(OH)_{n-}^{-}$  during OER, which effectively repel CI and enhance both the activity and corrosion resistance. These outstanding studies confirmed that surface-modified anions can effectively prevent Clfrom damaging the anodes. However, the relatively complex design of electrodes hinders large-scale application, and a gap still exists between theoretical research and industrial implementation of seawater electrolysis<sup>[20]–[25]</sup>.

In this study, we proposed a simple electrolyte engineering strategy by adding 0.25 M NaF into an alkaline simulated seawater electrolyte (denoted as ASSE, 1 M KOH + 0.5 M NaCl). The introduced F<sup>-</sup> facilitated surface reconstruction of the anode to boost OER activity, while simultaneously repelling Cl<sup>-</sup> to enhance corrosion resistance. This simple approach achieved effects comparable to those of complex electrode designs,

enabling the commonly used NiFe-LDH anode, typically lacking corrosion resistance, to operate stably for 1500 hours at 1 A cm<sup>-2</sup>. This work bridges the gap between theoretical research and practical application in the field of seawater electrolysis and holds promise for advancing its industrialization.

#### 2. Results

NiFe-based anodes have been proven to exhibit the most outstanding OER activity under alkaline conditions, and NiFe-LDH has long been considered one of the most promising candidates due to its facile synthesis. Here, a simple one-step hydrothermal method was employed to grow NiFe-LDH nanoarrays on a nickel foam substrate (Figure 1a)<sup>[26]</sup>. Based on previous studies, the Ni/Fe feeding ratio was controlled at 2/1 to achieve optimal catalytic performance<sup>[27],[28]</sup>.

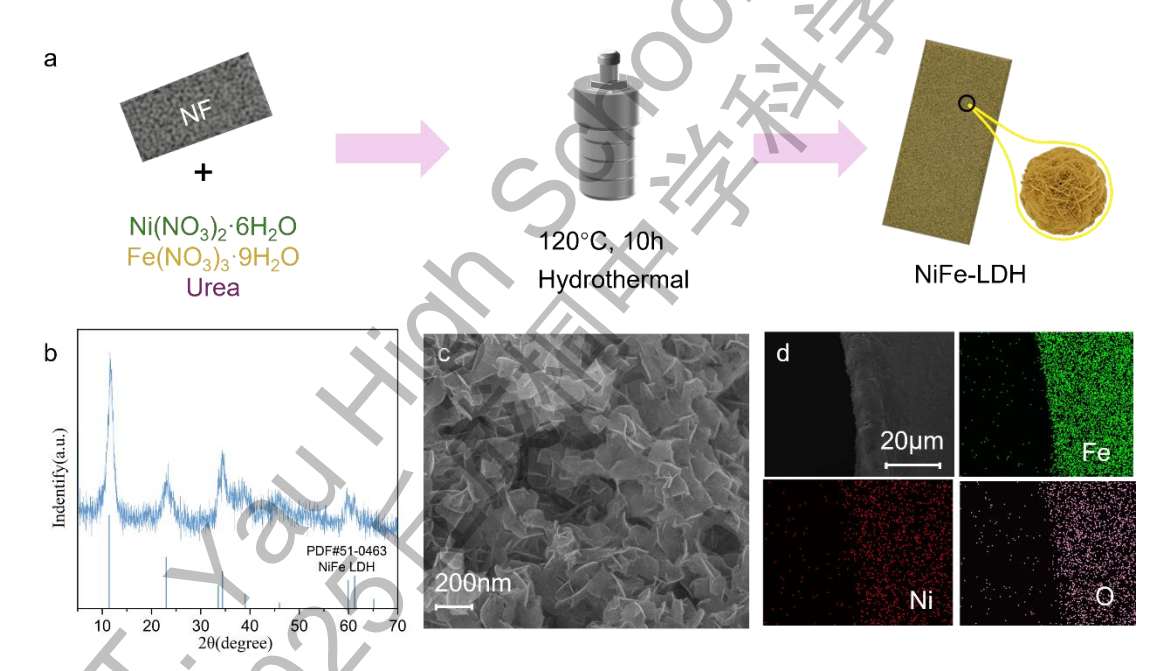


**Figure 1.** (a) Schematic route for the synthesis of NiFe-LDH. (b) XRD pattern, (c) SEM image, and (d) EDS elemental mapping of NiFe-LDH.

Figure 1b presents the X-ray diffraction (XRD) pattern of the NiFe-LDH nanoarrays exfoliated by ultrasonication, with the nickel foam substrate removed to avoid interference from its strong diffraction signals. The diffraction peaks at 11.5° and 23.3° correspond to the (003) and (006) planes, respectively, indicating the typical layered structure of NiFe-LDH<sup>[29],[30]</sup>. Other diffraction peaks also match well with the standard pattern (PDF#51-0463), further confirming that the lamellar structure corresponds to

NiFe-LDH with a Ni/Fe ratio of 2/1, thus demonstrating the successful preparation of the target structure<sup>[31]</sup>. The morphology of NiFe-LDH was examined by scanning electron microscopy (SEM, Figure 1c), the NiFe-LDH exhibits a network of interwoven nanosheets, each with a lateral size of less than 200 nm. This nanoscale architecture facilitates the full exposure of catalytic active sites and enhances electrode-electrolyte interaction due to the increased surface roughness, thereby improving wettability<sup>[32]–[35]</sup>. Furthermore, energy dispersive X-ray spectroscopy (EDS) elemental mapping confirmed the uniform distribution of Ni, Fe, and O throughout the material, indicating the homogeneous structure of the NiFe-LDH.

As illustrated in Figures 2a–b, NiFe-LDH exhibited an overpotential of around 251 mV to achieve 10 mA cm $^{-2}$  in ASSE, notably higher than the commonly reported  $\eta_{10}$  range of 190-230 mV. This degradation in activity suggests that Cl $^{-1}$  in the electrolyte was adsorbed onto the catalyst surface, thereby deactivating some of the active sites[36],[37]. With the introduction of NaF into ASSE, the performance of NiFe-LDH improved significantly, reaching its optimum at a NaF concentration of approximately 0.25 M, where  $\eta_{10}$  was reduced to around 222 mV. This value is close to the typical results mentioned earlier, indicating that the addition of NaF effectively mitigated the poisoning effect of Cl $^{-1}$ . It should be noted that the above electrochemical data were iR-corrected (R was determined by electrochemical impedance spectroscopy in Figure 2c, denoted as EIS), confirming that the performance enhancement was not caused by changes in solution resistance. Moreover, NaF was fully dissolved in the electrolyte, existing as Na $^+$  and F $^-$  ions. Since the anodic potential applied to the NiFe-LDH during operation exceeded its zero-charge point, the improved activity was mainly attributed to the effect of F $^-$ , rather than an increase in Na $^+$  concentration[38].

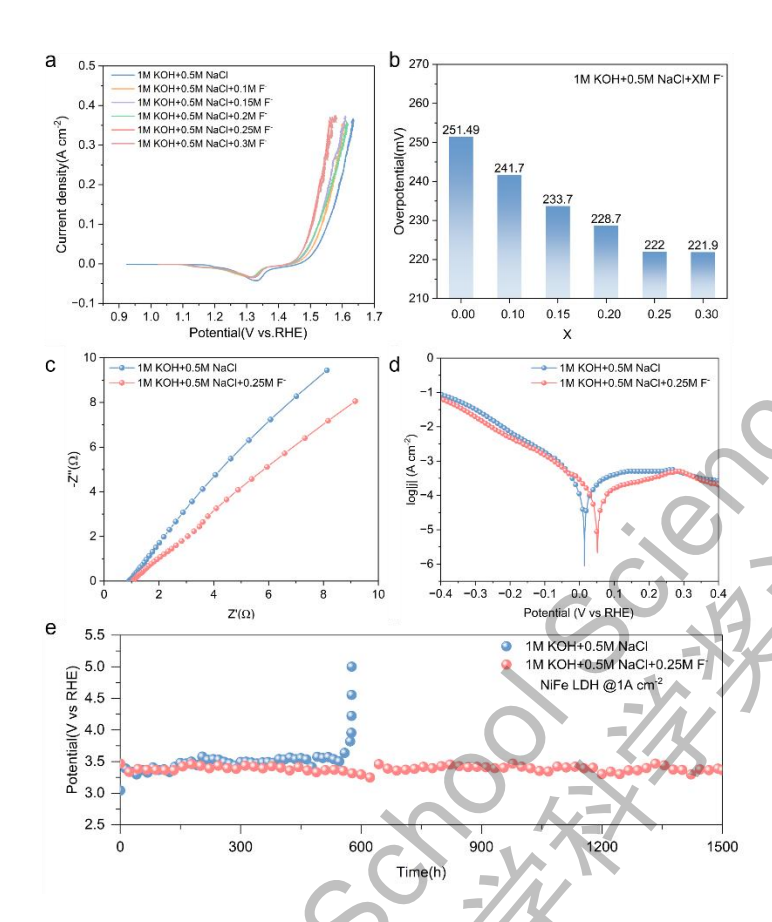


**Figure 2.** (a) Polarization curves and (b)  $\eta_{10}$  of NiFe-LDH as a function of NaF concentration. (c) EIS, (d) corrosion polarization curves, and (e) CP curves of NiFe-LDH at 1 A cm<sup>-2</sup> in the ASSE with/without 0.25 M F<sup>-</sup>.

Cl<sup>-</sup> corrosion on the anode can lead to complete deactivation of the electrolysis system, making corrosion resistance a critical parameter for seawater electrolysis anodes. As shown in the corrosion polarization curves (Figure 2d), the corrosion potential of NiFe-LDH increased from approximately 0 V to about 0.05 V vs RHE after introducing 0.25 M F<sup>-</sup> into the ASSE, confirming that F<sup>-</sup> contributed to enhanced corrosion resistance. The chrono-potential (CP) measurement in Figure 2e further confirmed this result. In ASSE containing F<sup>-</sup>, NiFe-LDH maintained stable operation at 1 A cm<sup>-2</sup> for 1500 hours, which is 2.5 times longer than the blank control. These results highlight the role of electrolyte engineering in improving the long-term durability of NiFe-LDH.

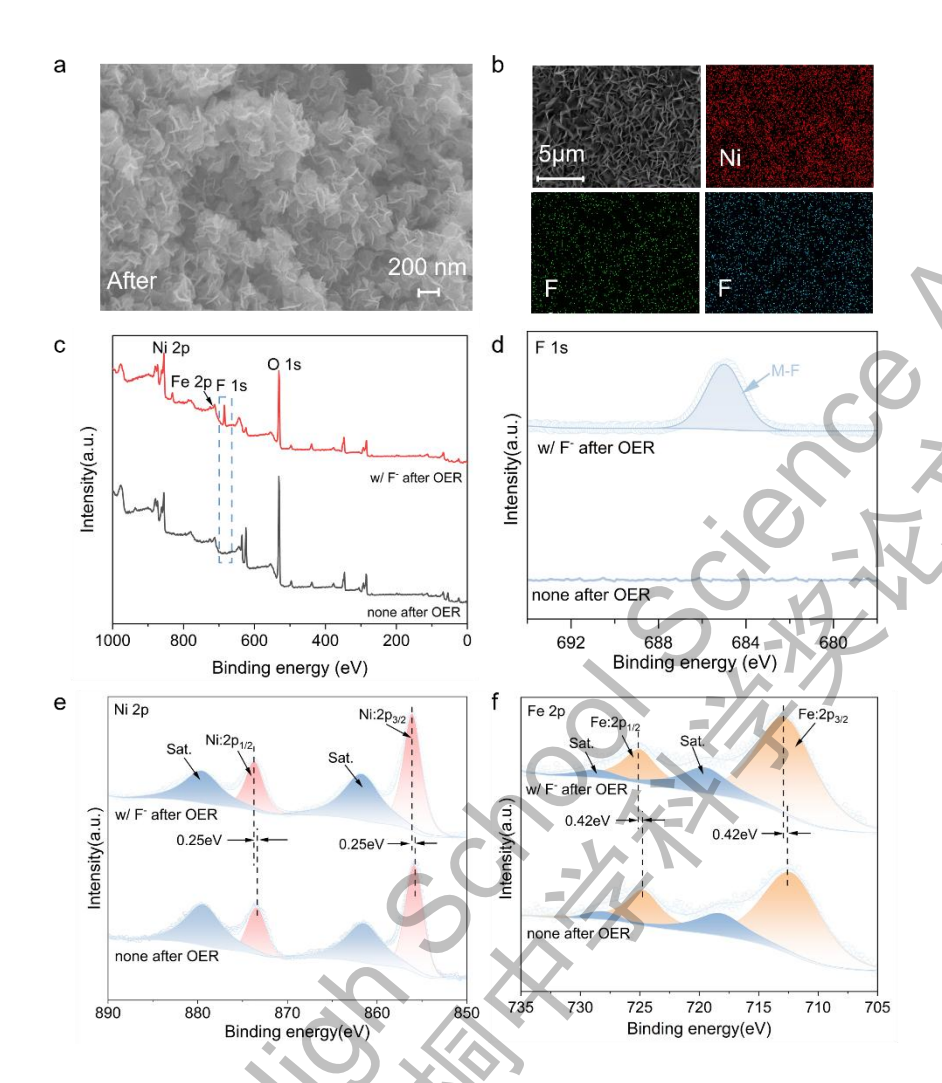


**Figure 3.** (a) SEM image, (b) EDS elemental mapping of NiFe-LDH post CP test in the ASSE with 0.25 M F<sup>-</sup>. (c) XPS survey, (d) F 1s XPS, (e) Ni 2p XPS, and (f) Fe 2p XPS of NiFe-LDH post CP test in the ASSE with/without 0.25 M F<sup>-</sup>.

Earlier investigations demonstrated that NiFe-LDH anodes experience dynamic dissolution and redeposition of metal sites during operation, often leading to structural degradation and impaired surface wettability<sup>[19],[38],[39]</sup>. Remarkably, as illustrated in Figure 3a, the NiFe-LDH retained its morphology with virtually no observable changes even after continuous operation at 1 A cm<sup>-2</sup> for 1500 hours. EDS elemental mapping results (Figure 3b) demonstrated the absence of phase separation in the electrode, highlighting a crucial factor behind the long-term stability of NiFe-LDH. Additionally, the uniform distribution of F species after CP testing indicated their adsorption on the NiFe-LDH surface. This was corroborated by X-ray photoelectron spectroscopy (XPS, Figure 3c-d) analysis, which showed a distinct peak near 685 eV, characteristic of

metal-fluoride coordination<sup>[40]</sup>.

Fluorine possesses the highest electronegativity, and its coordination with metal sites leads to electron redistribution within the material. High-resolution Ni 2p XPS spectra in Figure 3e revealed two pairs of signals corresponding to Ni<sup>2+</sup> (red peaks) and satellite peaks (blue peaks)<sup>[41]–[43]</sup>. Meanwhile, the signal assigned to Ni<sup>2+</sup> 2p<sub>3/2</sub> and 2p<sub>1/2</sub> both shifted to higher binding energy by 0.25 eV. Similar phenomenon can also be observed in Fe 2p XPS (yellow peaks in Figure 3f), where the peaks of Fe<sup>3+</sup> shifted 0.42 eV. These results indicate that F<sup>-</sup> adsorption decreased the electron density around the Ni/Fe sites<sup>[44]–[46]</sup>. Since high-valence Ni and Fe species formed during OER serve as active sites, the F<sup>-</sup>-induced electronic modulation accounted for the enhanced catalytic activity of NiFe-LDH.

In situ characterizations were conducted to evaluate the effect of F- on the behavior of NiFe-LDH during operation. As shown in Figure 4b, Bode plots of NiFe-LDH in 0.25 M F-containing ASSE revealed that structural reconstruction was reflected by phase angle changes in the middle-frequency region, whereas OER process was represented by shifts in the low-frequency range [47],[48]. At 1.42 V vs RHE, the middle-frequency peak declined sharply, indicating the electrooxidation of NiFe-LDH. Concurrently, a new peak appeared in the low-frequency region, associated with the formation of OER intermediates, which gradually faded as the applied potential increased, suggesting their consumption and the onset of OER around 1.44 V vs RHE<sup>[49],[50]</sup>. In contrast, in situ EIS of NiFe-LDH in F-free electrolyte displayed a similar spectral shape to that in Figure 4a but required a higher potential of 1.44 V vs RHE for electrooxidation and 1.46 V vs RHE to initiate OER, consistent with Figure 2a<sup>[51]</sup>. This comparison confirmed that the presence of F- promoted NiFe-LDH activation and improved OER kinetics. In situ Raman spectroscopy (Figure 4c-d) also yielded similar results, with the evolution of peaks in the 400-600 cm<sup>-1</sup> region indicating a more rapid reconstruction into Ni/Fe-OOH phases in the presence of F-[52],[53].

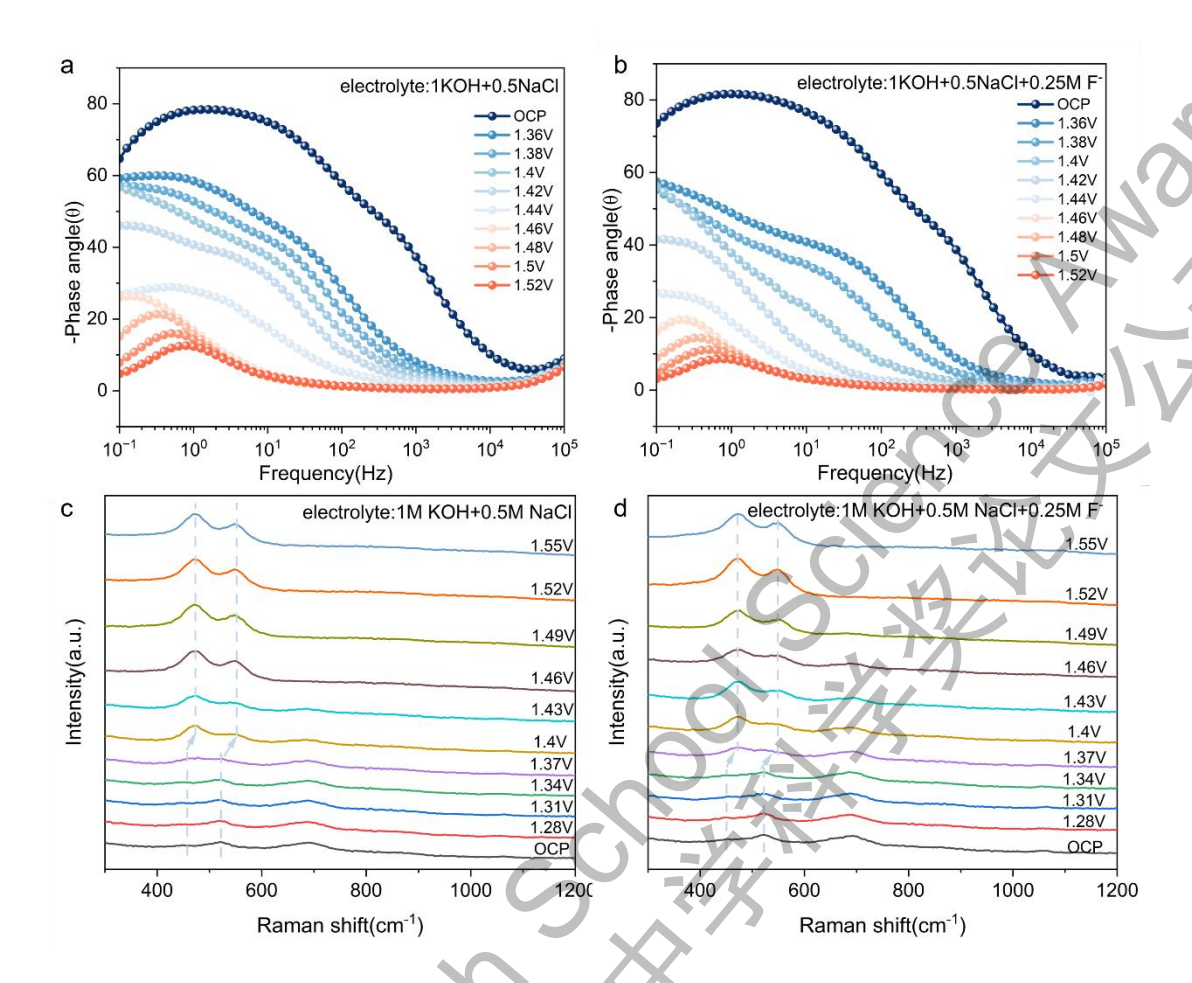


**Figure 4.** In situ EIS of NiFe-LDH in the ASSE (a) with and (b) without 0.25 M F<sup>-</sup>. In situ Raman of NiFe-LDH in the ASSE (c) with and (d) without 0.25 M F<sup>-</sup>.

The enhanced reconstruction kinetics of NiFe-LDH provided further evidence of the dynamic adsorption of F<sup>-</sup> during OER. Due to their extremely small ionic radius, F<sup>-</sup> exhibited highly localized negative charge, which is positively correlated with electrostatic repulsion against CI<sup>-</sup>[10],[54]. This means that under anodic potential, the adsorbed F<sup>-</sup> exerted strong repulsion toward CI<sup>-</sup>, thereby suppressing its attack on the electrode. As a result, the poisoning of active sites was avoided, and the corrosion resistance of the electrode was enhanced.

# 3. Conclusion

Seawater electrolysis enables efficient hydrogen production while conserving freshwater resources. However, Cl<sup>-</sup> in seawater can impair anode activity and cause severe corrosion, often necessitating complex anode designs, which poses challenges for industrial-scale implementation. In this work, F<sup>-</sup> was demonstrated to

serve as an effective electrolyte additive that enhances the activity of the NiFe layered double hydroxide (NiFe-LDH) anode while preventing corrosion. Upon optimizing the F<sup>-</sup> concentration, NiFe-LDH achieved stable operation at 1 A cm<sup>-2</sup> for 1500 hours in saline electrolyte, representing an approximately 2.5-fold improvement over the unprotected control. Characterizations demonstrated that F<sup>-</sup> adsorbed onto the NiFe-LDH surface during operation, inducing electron redistribution and facilitating rapid reconstruction, which enhanced OER performance. Its highly localized negative charge also provided strong electrostatic repulsion to block CI- attack, effectively shielding the electrode and greatly improving its stability. This electrolyte engineering approach combines ease of application with a clear mechanism and universal compatibility with various electrodes, presenting a promising pathway toward industrialization of seawater electrolysis.

# 4. Methods

#### 4.1 Chemicals and materials

Various chemicals were used in this study.  $Ni(NO_3)_2 \cdot 6H_2O$ ,  $Fe(NO_3)_3 \cdot 9H_2O$  were purchased from Aladdin Industrial Co. Urea, KOH, NaCl were purchased from Beijing Chemical Reagents Co. NaF was purchased from Shanghai Macklin Biochemical Co. Deionized water with a resistivity  $\geq 18$  M $\Omega$  was used to prepare all aqueous solutions. All the reagents were of analytical grade and were used directly without further purification.

# 4.2 Synthesis of NiFe LDHs electrode.

First, 0.66 mmol Ni(NO<sub>3</sub>)<sub>2</sub>·6H<sub>2</sub>O, 0.33 mmol Fe(NO<sub>3</sub>)<sub>3</sub>·9H<sub>2</sub>O, and 5 mmol urea were dissolved in 36 mL deionized water. Then this solution and a piece of 3\*4 cm<sup>2</sup> cleaned Ni foam was transferred into the Teflon-lined stainless autoclave and maintained at  $120^{\circ}$ C for 12 h to get the NiFe LDHs electrode.

## 4.3 Physical characterization

XRD patterns were recorded on an Ultima IV (Rigaku) in the range from 5° to 90° at a scan rate of 5°/min. SEM images were obtained on a Zeiss SUPRA55 scanning

electron microscope, which was operated at 10 kV. XPS were performed by using a model of K-Alpha (Thermo Scientific). ICP-OES and ICP-MS were carried out by the Thermo Fisher iCAP 7400.

#### 4.4 Electrochemical measurements

A three-electrode system was conducted to perform all electrochemical measurements under the temperature of 25°C. The obtained electrocatalyst (work surface area: 1 cm\*1 cm), Hg/HgO, and graphite rod were severed as the working electrode, reference electrode, and counter electrode, respectively. The measured potentials versus Hg/HgO could be converted to the potentials versus reversible hydrogen electrode (RHE) by Equation (1):

$$E_{RHE} = E_{Hg/HgO} + 0.098 + 0.059 \times pH$$
(1)

OER performance was tested in alkaline simulated seawater (1 M KOH + 0.5 M NaCl) and in alkaline simulated seawater with added halide ions (1 M KOH + 0.5 M NaCl + X<sup>-</sup>). The electrochemical behavior was investigated using reverse linear sweep voltammetry (LSV) from 1.8 to 0.1 V vs Hg/HgO at a scan rate of 5 mV s<sup>-1</sup>. The curves were manually corrected with 90% iR compensation. The R is obtained from electrochemical impedance spectroscopy (EIS), with the frequency range from 10<sup>5</sup> to 10<sup>-1</sup> Hz and an amplitude of 10 mV. Tafel slopes were obtained by plotting potential against log (j) from LSV curves. The corrosion behaviors (corrosion potential and corrosion current) of NiFe LDHs in alkaline simulated seawater with added halide ions were demonstrated by Tafel Plots.

# 4.5 In-situ electrochemical Raman measurements

Electrochemical Raman spectroscopy was carried out on a Horiba Lab RAM HR Evolution confocal Raman spectrometer with a 532 nm laser source, a 50×objective and an acquisition time of 90 s. And the electrochemical workstation (CHI 660D, Chenhua, Shanghai) were used to performed the Amperometric i-t Test under OCP to 1.52 vs RHE, respectively. Each spectrum was obtained at least three times with an

exposure time of 30 s.

# 5. Acknowledgements

The selection of this research topic stemmed from my interest in hydrogen energy and seawater electrolysis. Chloride-induced corrosion and electrode selectivity have long been critical challenges hindering the industrialization of seawater electrolysis. Therefore, I sought to explore the potential role of fluoride ions in the OER of seawater, with the aim of enhancing electrode activity and stability while contributing to the advancement of green hydrogen production.

During the course of this research, I received invaluable guidance from Professor Xiaoming Sun at Beijing University of Chemical Technology. He provided comprehensive and detailed support in research direction, experimental design, electrocatalytic principles, and data analysis. His mentorship was entirely voluntary, ensuring the scientific rigor and feasibility of the study, and greatly enhancing my research mindset and academic skills. I am deeply grateful to Professor Sun for offering me the opportunity to join the laboratory, conduct experiments, and learn essential concepts in this field.

My second mentor was Ms. Ejing Kong, my high school chemistry teacher at The High School Affiliated to Beijing Normal University, who gave me valuable advice during the writing stage of the research report. Her guidance helped me further refine the structure and logical expression of the paper. I sincerely thank both of my mentors for their selfless guidance, which significantly improved my academic development and way of thinking.

I would also like to express my special thanks to doctoral students Wei Liu and Jingjin Cheng from Professor Sun's group, who provided valuable guidance and suggestions during both the experimental process and the preparation of this paper.

The research topic was identified after I independently explored my area of interest and discussed it with Professor Sun. For the practical work, including literature review, experimental design, and data collection, I completed the tasks independently under my mentors' guidance, while part of the data analysis was assisted by Wei Liu and Jingjin Cheng. The paper was written entirely by myself.

Throughout this research journey, I have not only gained experimental skills and research experience but also cultivated a spirit of exploration and problem-solving ability. I am truly grateful to my mentors for their selfless support, as well as to everyone who has provided me with assistance and encouragement along the way.

### 6. References

- [1] Hassan, Q.; Viktor, P.; J. Al-Musawi, T.; Mahmood Ali, B.; Algburi, S.; Alzoubi, H. M.; Khudhair Al-Jiboory, A.; Zuhair Sameen, A.; Salman, H. M.; Jaszczur, M. The renewable energy role in the global energy Transformations. *Renew. Energy Focus* **2024**, *48*, 100545.
- [2] Turner, J. A. Sustainable Hydrogen Production. Science 2004, 305, 972–974.
- [3] Dresselhaus, M. S.; Thomas, I. L. Alternative energy technologies. *Nature* **2001**, *414*, 332–337.
- [4] Tong, W.; Forster, M.; Dionigi, F.; Dresp, S.; Sadeghi Erami, R.; Strasser, P.; Cowan, A. J.; Farràs, P. Electrolysis of low-grade and saline surface water. *Nat. Energy* **2020**, *5*, 367–377.
- [5] Saada, H.; Fabre, B.; Loget, G.; Benoit, G. Is Direct Seawater Splitting Realistic with Conventional Electrolyzer Technologies? *ACS Energy Lett.* **2024**, 3351–3368.
- [6] He, W.; Li, X.; Tang, C.; Zhou, S.; Lu, X.; Li, W.; Li, X.; Zeng, X.; Dong, P.; Zhang, Y.; Zhang, Q. Materials Design and System Innovation for Direct and Indirect Seawater Electrolysis. *ACS Nano* **2023**, *17*, 22227–22239.
- [7] Zhang, F.; Yu, L.; Wu, L.; Luo, D.; Ren, Z. Rational design of oxygen evolution reaction catalysts for seawater electrolysis. *Trends Chem.* **2021**, *3*, 485–498.
- [8] Ma, T.; Xu, W.; Li, B.; Chen, X.; Zhao, J.; Wan, S.; Jiang, K.; Zhang, S.; Wang, Z.; Tian, Z.; Lu, Z.; Chen, L. The Critical Role of Additive Sulfate for Stable Alkaline Seawater Oxidation on Nickel-Based Electrodes. *Angew. Chem. Int. Ed.* **2021**, *60*, 22740–22744.
- [9] Kuang, Y.; Kenney, M. J.; Meng, Y.; Hung, W.-H.; Liu, Y.; Huang, J. E.; Prasanna, R.; Li, P.; Li, Y.; Wang, L.; Lin, M.-C.; McGehee, M. D.; Sun, X.; Dai, H. Solar-driven, highly sustained splitting of seawater into hydrogen and oxygen fuels. *Proc. Natl. Acad. Sci.* **2019**, *116*, 6624–6629.
- [10] Liu, W.; Yu, J.; Sendeku, M. G.; Li, T.; Gao, W.; Yang, G.; Kuang, Y.; Sun, X. Ferricyanide Armed Anodes Enable Stable Water Oxidation in Saturated Saline Water

- at 2 A/cm2. Angew. Chem. Int. Ed. 2023, 62, e202309882.
- [11] He, X.; Yao, Y.; Zhang, L.; Wang, H.; Tang, H.; Jiang, W.; Ren, Y.; Nan, J.; Luo, Y.; Wu, T.; Luo, F.; Tang, B.; Sun, X. Hexafluorophosphate additive enables durable seawater oxidation at ampere-level current density. *Nat. Commun.* **2025**, *16*, 4998.
- [12] Liu, Y.; Li, L.; Li, X.; Xu, Y.; Wu, D.; Sakthivel, T.; Guo, Z.; Zhao, X.; Dai, Z. Asymmetric tacticity navigates the localized metal spin state for sustainable alkaline/sea water oxidation. *Sci. Adv.* **2025**, *11*, eads0861.
- [13] Li, T.; Zhao, X.; Getaye Sendeku, M.; Zhang, X.; Xu, L.; Wang, Z.; Wang, S.; Duan, X.; Liu, H.; Liu, W.; Zhou, D.; Xu, H.; Kuang, Y.; Sun, X. Phosphate-decorated Ni3Fe-LDHs@CoPx nanoarray for near-neutral seawater splitting. *Chem. Eng. J.* **2023**, *460*, 141413.
- [14] Hu, H.; Wang, X.; Attfield, J. P.; Yang, M. Metal nitrides for seawater electrolysis. *Chem. Soc. Rev.* **2024**, *53*, 163–203.
- [15] Yuan, W.; Wang, S.; Ma, Y.; Qiu, Y.; An, Y.; Cheng, L. Interfacial Engineering of Cobalt Nitrides and Mesoporous Nitrogen-Doped Carbon: Toward Efficient Overall Water-Splitting Activity with Enhanced Charge-Transfer Efficiency. *ACS Energy Lett.* **2020**, *5*, 692–700.
- [16] Yu, L.; Zhu, Q.; Song, S.; McElhenny, B.; Wang, D.; Wu, C.; Qin, Z.; Bao, J.; Yu, Y.; Chen, S.; Ren, Z. Non-noble metal-nitride based electrocatalysts for high-performance alkaline seawater electrolysis. *Nat. Commun.* **2019**, *10*, 5106.
- [17] Kang, X.; Yang, F.; Zhang, Z.; Liu, H.; Ge, S.; Hu, S.; Li, S.; Luo, Y.; Yu, Q.; Liu, Z.; Wang, Q.; Ren, W.; Sun, C.; Cheng, H.-M.; Liu, B. A corrosion-resistant RuMoNi catalyst for efficient and long-lasting seawater oxidation and anion exchange membrane electrolyzer. *Nat. Commun.* **2023**, *14*, 3607.
- [18] Chen, H.; Liu, P.; Li, W.; Xu, W.; Wen, Y.; Zhang, S.; Yi, L.; Dai, Y.; Chen, X.; Dai, S.; Tian, Z.; Chen, L.; Lu, Z. Stable Seawater Electrolysis Over 10 000 H via Chemical Fixation of Sulfate on NiFeBa-LDH. *Adv. Mater.* **2024**, 2411302.
- [19] Liu, W.; Yu, J.; Li, T.; Li, S.; Ding, B.; Guo, X.; Cao, A.; Sha, Q.; Zhou, D.; Kuang, Y.; Sun, X. Self-protecting CoFeAl-layered double hydroxides enable stable and efficient brine oxidation at 2 A cm-2. *Nat. Commun.* **2024**, *15*, 4712.
- [20] Niaz, H.; Lakouraj, M. M.; Liu, J. Techno-economic feasibility evaluation of a standalone solar-powered alkaline water electrolyzer considering the influence of battery energy storage system: A Korean case study. *Korean J. Chem. Eng.* **2021**, *38*, 1617–1630.
- [21] Kuleshov, N. V.; Kuleshov, V. N.; Dovbysh, S. A.; Grigoriev, S. A.; Kurochkin, S. V.; Millet, P. Development and performances of a 0.5 kW high-pressure alkaline water electrolyser. *Int. J. Hydrog. Energy* **2019**, *44*, 29441–29449.
- [22] Wang, N.; Song, S.; Wu, W.; Deng, Z.; Tang, C. Bridging Laboratory Electrocatalysts with Industrially Relevant Alkaline Water Electrolyzers. *Adv. Energy Mater.* **2024**, *14*, 2303451.
- [23] Ren, Z.; Wang, J.; Yu, Z.; Zhang, C.; Gao, S.; Wang, P. Experimental studies and modeling of a 250-kW alkaline water electrolyzer for hydrogen production. *J. Power Sources* **2022**, *544*, 231886.
- [24] David, M.; Ocampo-Martínez, C.; Sánchez-Peña, R. Advances in alkaline water

- electrolyzers: A review. J. Energy Storage 2019, 23, 392-403.
- [25] LeRoy, R. L. Industrial water electrolysis: Present and future. *Int. J. Hydrog. Energy* **1983**, *8*, 401–417.
- [26] Lu, Z.; Xu, W.; Zhu, W.; Yang, Q.; Lei, X.; Liu, J.; Li, Y.; Sun, X.; Duan, X. Three-dimensional NiFe layered double hydroxide film for high-efficiency oxygen evolution reaction. *Chem. Commun.* **2014**, *50*, 6479–6482.
- [27] Louie, M. W.; Bell, A. T. An Investigation of Thin-Film Ni–Fe Oxide Catalysts for the Electrochemical Evolution of Oxygen. *J. Am. Chem. Soc.* **2013**, *135*, 12329–12337.
- [28] Ou, Y.; Twight, L. P.; Samanta, B.; Liu, L.; Biswas, S.; Fehrs, J. L.; Sagui, N. A.; Villalobos, J.; Morales-Santelices, J.; Antipin, D.; Risch, M.; Toroker, M. C.; Boettcher, S. W. Cooperative Fe sites on transition metal (oxy)hydroxides drive high oxygen evolution activity in base. *Nat. Commun.* **2023**, *14*, 7688.
- [29] Zhou, D.; Wang, S.; Jia, Y.; Xiong, X.; Yang, H.; Liu, S.; Tang, J.; Zhang, J.; Liu, D.; Zheng, L.; Kuang, Y.; Sun, X.; Liu, B. NiFe Hydroxide Lattice Tensile Strain: Enhancement of Adsorption of Oxygenated Intermediates for Efficient Water Oxidation Catalysis. *Angew. Chem. Int. Ed.* **2019**, *58*, 736–740.
- [30] Hu, Y.; Shen, T.; Wu, Z.; Song, Z.; Sun, X.; Hu, S.; Song, Y.-F. Coordination Stabilization of Fe by Porphyrin-Intercalated NiFe-LDH Under Industrial-Level Alkaline Conditions for Long-Term Electrocatalytic Water Oxidation. *Adv. Funct. Mater.* **2025**, *35*, 2413533.
- [31] Corrigan, D. A. The Catalysis of the Oxygen Evolution Reaction by Iron Impurities in Thin Film Nickel Oxide Electrodes. *J. Electrochem. Soc.* **1987**, *134*, 377–384.
- [32] Xu, W.; Lu, Z.; Sun, X.; Jiang, L.; Duan, X. Superwetting Electrodes for Gas-Involving Electrocatalysis. *Acc. Chem. Res.* **2018**, *51*, 1590–1598.
- [33] Lu, Z.; Zhu, W.; Yu, X.; Zhang, H.; Li, Y.; Sun, X.; Wang, X.; Wang, H.; Wang, J.; Luo, J.; Lei, X.; Jiang, L. Ultrahigh Hydrogen Evolution Performance of Under-Water "Superaerophobic" MoS2 Nanostructured Electrodes. *Adv. Mater.* **2014**, *26*, 2683–2687.
- [34] Jeong, S.; Kim, U.; Lee, S.; Zhang, Y.; Son, E.; Choi, K.-J.; Han, Y.-K.; Baik, J. M.; Park, H. Superaerophobic/Superhydrophilic Multidimensional Electrode System for High-Current-Density Water Electrolysis. *ACS Nano* **2024**, *18*, 7558–7569.
- [35] Lu, Z.; Xu, W.; Ma, J.; Li, Y.; Sun, X.; Jiang, L. Superaerophilic Carbon-Nanotube-Array Electrode for High-Performance Oxygen Reduction Reaction. *Adv. Mater.* **2016**, *28*, 7155–7161.
- [36] Liu, W.; Guo, X.; Jiang, Z.; Yu, J.; Zhou, L.; Li, T.; Guo, Y.; Li, S.; Ding, B.; Wang, K.; Yang, Y.; Xin, H.; Zhou, D.; Kuang, Y.; Sun, X. Cl<sup>-</sup> Boosted Active and Stable Seawater Reduction on Pt/CoP Nanoarray Electrocatalysts. *Adv. Energy Mater.* **2024**, *15*, 2404978.
- [37] Liu, H.; Shen, W.; Jin, H.; Xu, J.; Xi, P.; Dong, J.; Zheng, Y.; Qiao, S.-Z. High-Performance Alkaline Seawater Electrolysis with Anomalous Chloride Promoted Oxygen Evolution Reaction. *Angew. Chem. Int. Ed.* **2023**, *62*, e202311674.
- [38] Liu, W.; Ding, X.; Cheng, J.; Jing, J.; Li, T.; Huang, X.; Xie, P.; Lin, X.; Ding, H.;

- Kuang, Y.; Zhou, D.; Sun, X. Inhibiting Dissolution of Active Sites in 80 °C Alkaline Water Electrolysis by Oxyanion Engineering. *Angew. Chem. Int. Ed.* **2024**, 63, e202406082.
- [39] Feng, C.; Wang, F.; Liu, Z.; Nakabayashi, M.; Xiao, Y.; Zeng, Q.; Fu, J.; Wu, Q.; Cui, C.; Han, Y.; Shibata, N.; Domen, K.; Sharp, I. D.; Li, Y. A self-healing catalyst for electrocatalytic and photoelectrochemical oxygen evolution in highly alkaline conditions. *Nat. Commun.* **2021**, *12*, 5980.
- [40] Hao, Y.; Kang, Y.; Wang, S.; Chen, Z.; Lei, C.; Cao, X.; Chen, L.; Li, Y.; Liu, Z.; Gong, M. Electrode/Electrolyte Synergy for Concerted Promotion of Electron and Proton Transfers toward Efficient Neutral Water Oxidation. *Angew. Chem. Int. Ed.* **2023**, *62*, e202303200.
- [41] Guo, P.; Cao, S.; Huang, W.; Lu, X.; Chen, W.; Zhang, Y.; Wang, Y.; Xin, X.; Zou, R.; Liu, S.; Li, X. Heterojunction-Induced Rapid Transformation of Ni3+/Ni2+ Sites which Mediates Urea Oxidation for Energy-Efficient Hydrogen Production. *Adv. Mater.* **2024**, *36*, 2311766.
- [42] Xiang, L.; Zhang, W.-D.; Xu, H.; Hu, M.; Yang, J.; Liu, J.; Gu, Z.-G.; Yan, X. Hierarchical microspheres constructed by hexagonal NiCo(OH)2 nanosheets with rich Ni3+ species and carboxylic groups for efficient urea oxidation reaction. *J. Alloys Compd.* **2023**, 930, 167453.
- [43] Zhang, L.; Wang, L.; Lin, H.; Liu, Y.; Ye, J.; Wen, Y.; Chen, A.; Wang, L.; Ni, F.; Zhou, Z.; Sun, S.; Li, Y.; Zhang, B.; Peng, H. A Lattice-Oxygen-Involved Reaction Pathway to Boost Urea Oxidation. *Angew. Chem.* **2019**, *131*, 16976–16981.
- [44] Li, P.; Duan, X.; Kuang, Y.; Li, Y.; Zhang, G.; Liu, W.; Sun, X. Tuning Electronic Structure of NiFe Layered Double Hydroxides with Vanadium Doping toward High Efficient Electrocatalytic Water Oxidation. *Adv. Energy Mater.* **2018**, *8*, 1703341.
- [45] Lu, Z.; Qian, L.; Tian, Y.; Li, Y.; Sun, X.; Duan, X. Ternary NiFeMn layered double hydroxides as highly-efficient oxygen evolution catalysts. *Chem. Commun.* **2016**, *52*, 908–911.
- [46] Yu, J.; Huang, D.; Zhou, L.; Liu, W.; Zhou, D. Nb5+ doping induces cascading optimization effects in NiFe layered double hydroxides for efficient water oxidation. *J. Power Sources* **2025**, *647*, 237341.
- [47] Guo, L.; Chi, J.; Cui, T.; Zhu, J.; Xia, Y.; Guo, H.; Lai, J.; Wang, L. Phosphorus Defect Mediated Electron Redistribution to Boost Anion Exchange Membrane-Based Alkaline Seawater Electrolysis. *Adv. Energy Mater.* **2024**, *14*, 2400975.
- [48] Xiao, Z.; Huang, Y.-C.; Dong, C.-L.; Xie, C.; Liu, Z.; Du, S.; Chen, W.; Yan, D.; Tao, L.; Shu, Z.; Zhang, G.; Duan, H.; Wang, Y.; Zou, Y.; Chen, R.; Wang, S. *Operando* Identification of the Dynamic Behavior of Oxygen Vacancy-Rich Co  $_3$  O  $_4$  for Oxygen Evolution Reaction. *J. Am. Chem. Soc.* **2020**, *142*, 12087–12095.
- [49] Zhao, S.; Wang, Y.; Hao, Y.; Yin, L.; Kuo, C.-H.; Chen, H.-Y.; Li, L.; Peng, S. Lewis Acid Driving Asymmetric Interfacial Electron Distribution to Stabilize Active Species for Efficient Neutral Water Oxidation. *Adv. Mater.* **2024**, *36*, 2308925.
- [50] Zhou, S.; He, H.; Li, J.; Ye, Z.; Liu, Z.; Shi, J.; Hu, Y.; Cai, W. Regulating the Band Structure of Ni Active Sites in Few-Layered Nife-LDH by In Situ Adsorbed Borate for Ampere-Level Oxygen Evolution. *Adv. Funct. Mater.* **2024**, *34*, 2313770.

- [51] Zhang, N.; Hu, Y.; An, L.; Li, Q.; Yin, J.; Li, J.; Yang, R.; Lu, M.; Zhang, S.; Xi, P.; Yan, C.-H. Surface Activation and Ni-S Stabilization in NiO/NiS2 for Efficient Oxygen Evolution Reaction. *Angew. Chem.* **2022**, *134*, e202207217
- [52] Kim, J.-C.; Kim, D.-W. Enhanced hydrogen evolution activities of the hollow surface-oxidized cobalt phosphide nanofiber electrocatalysts in alkaline media. *Int. J. Energy Res.* **2022**, *46*, 13035–13043.
- [53] Qiu, Z.; Ma, Y.; Edvinsson, T. In operando Raman investigation of Fe doping influence on catalytic NiO intermediates for enhanced overall water splitting. *Nano Energy* **2019**, *66*, 104118.
- [54] Yu, M.; Li, J.; Liu, F.; Liu, J.; Xu, W.; Hu, H.; Chen, X.; Wang, W.; Cheng, F. Anionic formulation of electrolyte additive towards stable electrocatalytic oxygen evolution in seawater splitting. *J. Energy Chem.* **2022**, 72, 361–369.